www.jcrph.com
Journal of Cancer Research and Pharmacology. 2025; 1(2): 89-100
https://doi.org/10.22034/jcrph.2025.559607.1015

Research Article Open Access

Curcumin-mediated modulation of miR-21-5p and miR-126-3p enhances PTEN expression and suppresses VEGF in CaSki cell line

Parvin Mohammadi [1*]

[1] Department of Plant Biology, Faculty of Natural Sciences, University of Tabriz, Tabriz, Iran

[*] **Corresponding author: Parvin Mohammadi**. Department of Plant Biology, Faculty of Natural Sciences, University of Tabriz, Tabriz, Iran
Email: mpari7413@gmail.com

Received: 14 September 2025 **Revised:** 13 November 2025 **Accepted:** 16 November 2025 **e-Published:** 1 December 2025

Abstract

Background and Aims: Curcumin, a natural polyphenolic compound from Curcuma longa, exhibits anti-cancer properties by modulating miRNAs and targeting pathways like PI3K/Akt and angiogenesis. This study investigates the effects of curcumin on the expression of miR-21-5p, miR-210-3p, miR-126-3p, and miR-214-3p in HPV-16-positive CaSki cervical cancer cells, and their correlations with PTEN and VEGF.

Methods: CaSki cells were cultured and treated with curcumin at a sub-IC50 concentration (80 µM) for 48 hours, determined via MTT assay (IC50 = 96 µM). Total RNA was extracted using TRIzol, and qRT-PCR was used to assess PTEN, VEGF (normalized to GAPDH), and miRNA expression (normalized to U6). Data from nine biological replicates per group were analyzed using Welch's t-test for comparisons and Pearson's correlation for relationships.

Results: Curcumin significantly upregulated PTEN (1.861 ± SD, p=0.004; ~3.6-fold) and downregulated VEGF (-2.137 ± SD, p=0.006; ~0.23-fold). miRNA modulation included a trend toward miR-21-5p downregulation (-1.024 ± SD, p=0.057; ~0.48-fold), no change in miR-210-3p (p=0.344), and upregulation of miR-126-3p (1.674 ± SD, p=0.003; ~3.2-fold) and miR-214-3p (1.669 ± SD, p=0.019; ~3.2-fold). Correlations revealed miR-21-5p negatively associated with PTEN (r=-0.51, p=0.03) and positively with VEGF (r=0.57, p=0.01); miR-126-3p positively with PTEN (r=0.41, p=0.09) and negatively with VEGF (r=-0.49, p=0.03); miR-214-3p negatively with PTEN (r=-0.36, p=0.14).

Conclusions: Curcumin epigenetically modulates miRNAs in CaSki cells, enhancing PTEN and suppressing VEGF through regulatory networks involving miR-21-5p and miR-126-3p. These findings elucidate curcumin's anti-cancer mechanisms and support its potential as an adjunctive therapy for cervical cancer, warranting further in vivo validation.

Keywords: Curcumin, microRNAs, Cervical cancer.

Introduction

Cervical cancer remains a major global health concern, ranking as the fourth most common malignancy among women worldwide. Recent estimates indicate that, in 2022, approximately 662,301 new cases and 348,874 deaths were reported, with the burden disproportionately concentrated in low- and middle-income countries, where access to screening and vaccination programs remains limited. Projections suggest that, if current trends persist, the incidence of cervical cancer could increase by 56.8% and mortality by 80.7% by 2050, highlighting the urgent need for novel therapeutic strategies.[1-3] Human papillomavirus (HPV) infection, particularly with high-risk strains such as HPV-16, is the primary etiological factor; however, the transition from precancerous lesions to invasive carcinoma involves complex molecular changes, including dysregulation of oncogenic signaling pathways and epigenetic alterations.[4-8] Conventional treatment modalities, including surgery, radiotherapy, and chemotherapy, have improved survival rates for early-stage disease. However, advanced or recurrent cervical cancer often demonstrates resistance to these therapies, emphasizing the limitations of current regimens and the necessity for targeted therapies with reduced toxicity.[1-3,9-11]

In this context, natural compounds exhibiting multifaceted anti-cancer properties have garnered significant interest. Curcumin, a polyphenolic compound derived from the rhizome of *Curcuma longa* (turmeric), has been extensively studied for its chemopreventive and therapeutic potential across various malignancies, including cervical cancer. Curcumin exerts its therapeutic effects through multiple mechanisms, such as inducing apoptosis, inhibiting cell proliferation, suppressing invasion and metastasis, and modulating angiogenesis by targeting critical signaling pathways, including PI3K/Akt, NF-κB, and MAPK.[12-15] Emerging evidence also suggests that curcumin can influence epigenetic regulators, particularly microRNAs (miRNAs), which are small non-coding RNAs (~18–25 nucleotides) that post-transcriptionally modulate gene expression by binding to the 3'-untranslated regions (3'-UTRs) of target mRNAs, thereby inducing their degradation or translational repression. Dysregulated miRNAs play pivotal roles in cervical carcinogenesis, acting as oncomiRs (oncogenic miRNAs) or tumor suppressors.[16-18] Curcumin's ability to restore miRNA homeostasis has been associated with its anti-tumor efficacy.[14,19]

Among the miRNAs implicated in cervical cancer, miR-21-5p is a well-characterized oncomiR, frequently overexpressed in HPV-infected cervical tissues. miR-21-5p has been linked to enhanced proliferation, invasion, and resistance to apoptosis through the targeting of tumor suppressors such as phosphatase and tensin homolog (PTEN).[20,21] miR-210-3p, which is induced under hypoxic conditions, promotes angiogenesis and metastasis by regulating vascular endothelial growth factor (VEGF) and other hypoxia-responsive genes, thereby contributing to tumor progression in cervical cancer.[22-24] Conversely, miR-126-3p acts as a tumor suppressor by inhibiting VEGF-mediated angiogenesis and reducing cell migration and invasion.[25-28] Its downregulation is associated with poor prognosis in cervical malignancies. miR-214-3p exhibits a dual role, often being upregulated in cervical cancer, where it targets PTEN and facilitates epithelial-to-mesenchymal transition (EMT), thus promoting metastasis.[29-31] These miRNAs converge on critical pathways, including the PTEN/PI3K/Akt axis, which negatively regulates cell survival and proliferation, and VEGF-driven angiogenesis, a hallmark of tumor growth and metastasis.[32]

Curcumin's efficacy in cervical cancer models, such as HPV-16-positive CaSki cells, where it inhibits tumor growth and angiogenesis in xenografts by downregulating VEGF, COX-2, and EGFR.[15,33,34] Additionally, curcumin has been shown to modulate miRNA expression, including the downregulation of miR-21 in various cancers, leading to the upregulation of PTEN and inhibition of Akt signaling, thereby promoting apoptosis and reducing cellular proliferation. However, the specific effects of curcumin on miR-21-5p, miR-210-3p, miR-126-3p, and miR-214-3p in cervical cancer, as well as their predictive correlations with PTEN and VEGF, remain underexplored. This gap in knowledge is critical, as these miRNAs collectively influence the PTEN/PI3K/Akt/VEGF axis, a central pathway in cervical cancer progression.

Objectives

The present study aims to investigate the curcumin-mediated modulation of miR-21-5p, miR-210-3p, miR-126-3p, and miR-214-3p in HPV-16-positive CaSki cervical cancer cells, and to assess their predictive correlations with PTEN and VEGF expression. By elucidating these interactions, this research seeks to provide mechanistic insights into curcumin's anti-cancer effects and to support its potential as an adjunctive therapeutic agent for cervical cancer.

Methods

Cell Culture

The human epidermoid cervical carcinoma cell line, CaSki, which is HPV-16-positive (ATCC CRL-1550), was procured from the American Type Culture Collection (ATCC). Cells were cultured in RPMI-1640 medium (ATCC 30-2001), supplemented with 10% heat-inactivated fetal bovine serum (FBS; ATCC 30-2020), 100 U/mL penicillin, and 100 µg/mL streptomycin. The cells were incubated in a humidified atmosphere at 37°C with 5% CO_2. Subculturing occurred every 2 to 3 days, once cells reached 70-80% confluence, by gentle pipetting after detachment with 0.25% trypsin-EDTA. The cells were

subcultured at a ratio ranging from 1:3 to 1:6 into fresh complete medium (6.0–8.0 mL per flask). All experiments were conducted using cells between passages 5 and 15 to ensure phenotypic consistency and minimize genetic drift. For cryopreservation, stocks were thawed by placing vials in a 37°C water bath for 1-2 minutes, followed by immediate transfer to pre-warmed complete medium (8-10 mL) in a 15 mL centrifuge tube. The mixture was gently mixed and centrifuged at 300 × g for 5 minutes at room temperature to remove dimethyl sulfoxide (DMSO). Cell viability was assessed using trypan blue exclusion, with only stocks demonstrating >90% viable cells used in experiments. Mycoplasma contamination was monitored routinely using PCR-based detection kits, and all cultures tested negative throughout the study.

Curcumin Preparation and Treatment

Curcumin (Sigma-Aldrich, C1386, ≥94% purity) was dissolved in sterile dimethyl sulfoxide (DMSO; Sigma-Aldrich, D2650) to create a 10–40 mM stock solution by vortexing at room temperature until fully dissolved. The solution was aliquoted and stored at -20°C, shielded from light to prevent degradation. For treatments, the stock solution was thawed, serially diluted in complete RPMI-1640 medium to achieve the desired final concentrations, ensuring that the DMSO concentration did not exceed 0.1% (v/v) to avoid vehicle-induced cytotoxicity. Control groups received equivalent volumes of DMSO in medium. For molecular assays, cells were treated with a sub-IC50 concentration of 80 μM curcumin for 48 hours, as determined by preliminary dose-response curves, to induce molecular changes without substantial cell death.

MTT Assay for Cell Viability

Cell viability was determined using the 3-(4,5-dimethylthiazol-2-yl)-2,5-diphenyltetrazolium bromide (MTT) assay, which measures metabolic activity as a surrogate for cell proliferation and cytotoxicity. CaSki cells were seeded in sterile 96-well plates at a density of 5 × 10^3 cells per well in 100 μL of complete medium and allowed to adhere overnight at 37°C. Following this, the cells were treated with serial two-fold dilutions of curcumin (ranging from 0–1024 μM) in triplicate wells for 48 hours. After the treatment period, 10 μL of MTT solution (5 mg/mL in sterile phosphate-buffered saline [PBS]; Sigma-Aldrich, M5655) was added to each well. The plates were then incubated at 37°C for 4 hours to allow NAD(P)H-dependent oxidoreductase enzymes to reduce MTT to purple formazan crystals. After incubation, the medium was carefully aspirated, and 100 μL of DMSO was added to each well to dissolve the crystals. The plates were gently shaken for 10 minutes at room temperature, and absorbance was measured at 570 nm (test wavelength) with a reference subtraction at 630 nm using a microplate reader (Bio-Rad, Model 680). Cell viability was calculated as a percentage of untreated controls using the formula:

Viability (%)=(Absorbance treated/Absorbance control)×100

The IC50 value was derived through non-linear regression analysis in GraphPad Prism software (version 9.0), fitting the data to a four-parameter log(inhibitor) vs. normalized response curve, with the goodness of fit determined by $R^2 > 0.95$.

RNA Extraction

Total RNA, including small RNAs, was isolated from CaSki cells (both untreated and curcumin-treated) using TRIzol reagent (Invitrogen, 15596026), following the manufacturer's optimized protocol for high-quality RNA extraction from cell cultures. Briefly, 1 × 10^6 cells were lysed in 1 mL TRIzol by repeated pipetting and incubated at room temperature for 5 minutes to dissociate nucleoprotein complexes. The lysates were then mixed with 0.2 mL chloroform per 1 mL TRIzol and shaken vigorously for 15 seconds. After incubating at 15–30°C for 2–3 minutes, samples were centrifuged at 12,000 × g for 15 minutes at 4°C to achieve phase separation. The upper aqueous phase (~0.5 mL) was transferred to a fresh tube, mixed with 0.5 mL isopropanol per 1 mL TRIzol, incubated at room temperature for 10 minutes, and centrifuged at 12,000 × g for 10 minutes at 4°C to precipitate RNA. The RNA pellet was washed twice with 1 mL 75% ethanol (prepared with RNase-free water), centrifuged at 7,500 × g for 5 minutes at 4°C, and air-dried for 5–10 minutes. The RNA pellet was then resuspended in 20–50 μL RNase-free water by heating at 55–60°C for 10 minutes, if necessary. RNA concentration, purity, and integrity were determined using a NanoDrop 2000 spectrophotometer (Thermo Fisher Scientific), ensuring A260/A280 ratios of 1.8–2.1 and A260/A230 ratios >1.8.

Total RNA yields typically ranged from 5–10 µg per 10^6 cells. RNA integrity was further verified through 1% agarose gel electrophoresis, confirming sharp 18S and 28S rRNA bands with a 2:1 intensity ratio. RNA samples were aliquoted and stored at -80°C until further analysis to prevent degradation.

cDNA Synthesis and qRT-PCR for Gene Expression

First-strand complementary DNA (cDNA) was synthesized from 1 µg of total RNA using the High-Capacity cDNA Reverse Transcription Kit (Applied Biosystems, 4368814), utilizing random hexamer primers for comprehensive mRNA transcript coverage. Reactions (20 µL) were prepared on ice, containing 2× RT master mix (which includes MultiScribe™ Reverse Transcriptase, RNase inhibitor, dNTPs, and buffer), and incubated at 25°C for 10 minutes (primer annealing), followed by 37°C for 120 minutes (extension), and 85°C for 5 minutes (enzyme inactivation), then held at 4°C. cDNA was stored at -20°C or used immediately. Quantitative real-time PCR (qRT-PCR) was performed using Power SYBR Green PCR Master Mix (Applied Biosystems, 4309155) on a QuantStudio 6 Flex Real-Time PCR System (Applied Biosystems) to detect gene expression. Reactions (20 µL) contained 10 µL of 2× master mix (including SYBR Green I dye, AmpliTaq Gold DNA Polymerase, dNTPs with dUTP, and optimized buffer), 1 µL of cDNA (diluted 1:10), 0.5 µM each forward and reverse primer, and nuclease-free water. The thermal cycling conditions included an initial denaturation at 95°C for 10 minutes, followed by 40 cycles of 95°C for 15 seconds (denaturation) and 60°C for 60 seconds (annealing/extension), concluding with a final melt curve analysis from 60–95°C at 0.15°C/second to confirm the specificity of the amplicons. Primer efficiencies were validated at 90–110% using standard curves derived from serial cDNA dilutions. Gene expression levels were normalized to GAPDH and analyzed using the $2^{(-\Delta\Delta Ct)}$ method. All reactions were conducted in technical triplicate, with 9 biological replicates per group. The primer sequences are provided in Table 1.

Table 1. Primers for Genes (PTEN, VEGF, and GAPDH)

Gene	Forward Primer (5' to 3')	Reverse Primer (5' to 3')	Amplicon Size (bp)	Approximate Tm (°C)	Ref
PTEN	ACCAGGACCAGAGGAAACCT	GCTAGCCTCTGGATTTGACG	~150	60	[60]
VEGF	GAGATGAGCTTCCTACAGCAC	TCACCGCCTCGGCTTGTCACAT	~120	60	[61]
GAPDH	ACCCACTCCTCCACCTTTGAC	TGTTGCTGTAGCCAAATTCGTT	~100	60	[62]

cDNA Synthesis and qRT-PCR for miRNA Expression

miRNA-specific cDNA was synthesized from 10 ng of total RNA using the miRCURY LNA RT Kit (QIAGEN, 339340), which utilizes universal polyadenylation and looped reverse transcription (RT) primers for the strand-specific, sensitive detection of mature miRNAs. The reactions (10 µL) contained RNA, 5× reaction buffer, enzyme mix, and nuclease-free water. The reaction was incubated at 42°C for 60 minutes (polyadenylation and RT), followed by 95°C for 5 minutes (inactivation), and held at 4°C. The cDNA was diluted 1:60 for subsequent qPCR analysis. Quantitative RT-PCR was performed using the miRCURY LNA SYBR Green PCR Kit (QIAGEN, 339345) on the QuantStudio 6 Flex system, utilizing locked nucleic acid (LNA)-enhanced primers for high specificity and reduced off-target amplification. Reactions (10 µL) consisted of 5 µL of 2× master mix, 1 µL of diluted cDNA, 1 µL of the LNA PCR primer mix (pre-optimized for each target), and nuclease-free water. Thermal cycling conditions included an initial activation at 95°C for 2 minutes, followed by 40 cycles of 95°C for 10 seconds (denaturation) and 56°C for 60 seconds (annealing/extension), with a final melt curve analysis from 60–95°C at 0.05°C/second. Primer efficiencies were maintained between 90% and 110%, with melt curves showing single peaks, confirming amplicon specificity. Expression levels were normalized to U6 using the $2^{(-\Delta\Delta Ct)}$ method. All reactions were performed with 9 biological replicates per group, each in technical triplicate. The primer sequences are provided in Table 2.

Table 2. Primers for miRNAs (miR-21-5p, miR-210-3p, miR-126-3p, miR-214-3p) and U6 snRNA

miRNA /U6	RT Primer (5' to 3')	Forward Primer (5' to 3')	Reverse Primer (5' to 3')	Amplicon Size (bp)	Approximate Tm (°C)	Ref
miR-21-5p	CTCAACTGGTGTCGTGGAGTCG GCAATTCAGTTGAGCGTCAAC	CTCAACTGGTGTCGT GGAGT	TCGGCAGGTAGCT TATCAGACTGAT	~70	60	[63]
miR-210-3p	CTCAACTGGTGTCGTGGAGTCG GCAATTCAGTTGAGCTCAGCC	CTCAACTGGTGTCGT GGAGT	TCGGCAGGCTGTG CGTGTGACAGCG	~70	60	[64, 65]
miR-126-3p	CTCAACTGGTGTCGTGGAGTCG GCAATTCAGTTGAGCGCATTAT	ACACTCCAGCTGGGT CGTACCGTGAGTAAT	GTGCAGGGTCCGA GGT	~65	60	[66]
miR-214-3p	CCTGTTGTCTCCAGCCACAAAA GAGCACAATATTTCAGGAGAC AACAGGACTGCCT	CGGGCACAGCAGGC ACAGAC	CAGCCACAAAAGG CACAAT	~75	60	[67]
U6 snRNA	Not applicable (standard	CTCGCTTCGGCAGCA CAT	TTTGCGTGTCATCC TTGCG			[68]

Statistical Analysis

Data analysis was conducted using GraphPad Prism software (version 9.0; GraphPad Software, Inc.). Normality of distributions was assessed via the Shapiro-Wilk test on log2-transformed fold changes. Comparisons between groups (untreated vs. treated) were made using Welch's t-test to account for unequal variances, with a significance threshold set at $p < 0.05$. Correlations between miRNA and gene expression levels were evaluated using Pearson's correlation coefficient on the combined dataset (n=18), and both p-values and r coefficients were reported. Results are presented as the mean ± standard deviation (SD), with fold changes calculated as log2-transformed values relative to controls. No outliers were excluded without justification, and power analysis confirmed that the sample size (n=9) was sufficient to detect effect sizes >1.5 with 80% power at $\alpha = 0.05$.

Results

Determination of Curcumin IC50 in CaSki Cells

To assess the cytotoxic effects of curcumin on HPV-16-positive CaSki cervical cancer cells, a dose-response analysis was conducted using the MTT assay following 48 hours of exposure. Cell viability exhibited a concentration-dependent decrease, ranging from 100% at 0 µM to nearly 0% at 1024 µM [Figure 1]. The calculated half-maximal inhibitory concentration (IC50) was 96 µM, with a strong fit to the log(inhibitor) vs. response curve ($R^2 = 0.98$). This value is consistent with previously reported IC50 ranges for curcumin in cervical cancer cell lines, where concentrations between 30-100 µM are commonly associated with anti-proliferative effects. For subsequent experiments, a sub-IC50 concentration of curcumin was used to examine molecular alterations without inducing significant cytotoxicity.

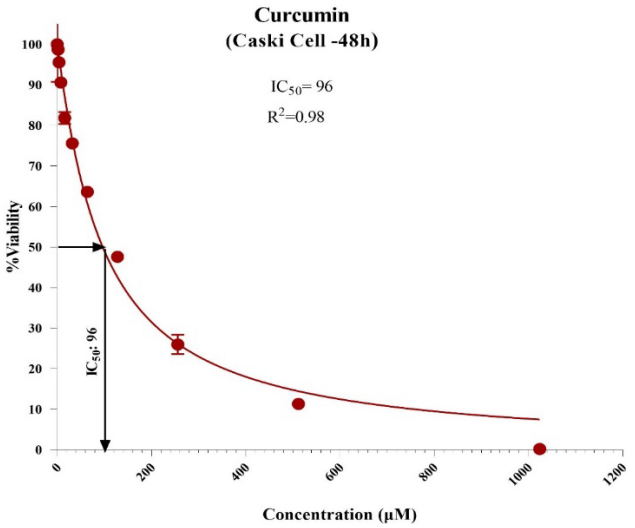

Figure-1. Dose-response curve illustrating the concentration- dependent inhibition of CaSki cervical cancer cell viability by curcumin following 48 hours of exposure, as assessed via MTT assay, with data points representing mean viability percentages from triplicate experiments fitted to a non-linear regression model. The calculated half-maximal inhibitory concentration (IC50) is 96 µM, demonstrating strong curve fit ($R^2 = 0.98$) and highlighting curcumin's cytotoxic potential in this HPV-16-positive cell line.

Curcumin-Induced Changes in PTEN and VEGF Gene Expression

Quantitative real-time PCR (qRT-PCR) was utilized to evaluate the effect of curcumin treatment on the expression of PTEN, a critical tumor suppressor gene involved in apoptosis, and VEGF, a pro-angiogenic factor that promotes cell proliferation. The expression data were

normalized to GAPDH, a housekeeping gene, and presented as log2 fold changes. For PTEN, the mean log2 fold change in untreated cells was -0.047±SD (from 9 replicates), whereas curcumin-treated cells showed a mean log2 fold change of 1.861±SD (p=0.004, Welch's t-test) [Figure 2A]. This corresponds to a significant upregulation, approximately a 3.6-fold increase in PTEN mRNA levels following curcumin treatment. In contrast, VEGF expression in untreated cells yielded a mean log2 fold change of 0.438 ± SD, while curcumin-treated cells exhibited a marked downregulation with a mean log2 fold change of -2.137 ± SD (p = 0.006, Welch's t-test) [Figure 2B], corresponding to a reduction to approximately 0.23-fold of the untreated levels. These results indicate a suppression of angiogenic potential, consistent with curcumin's well-documented influence on signaling pathways such as PI3K/Akt, where PTEN acts as a negative regulator and VEGF serves as a downstream effector.

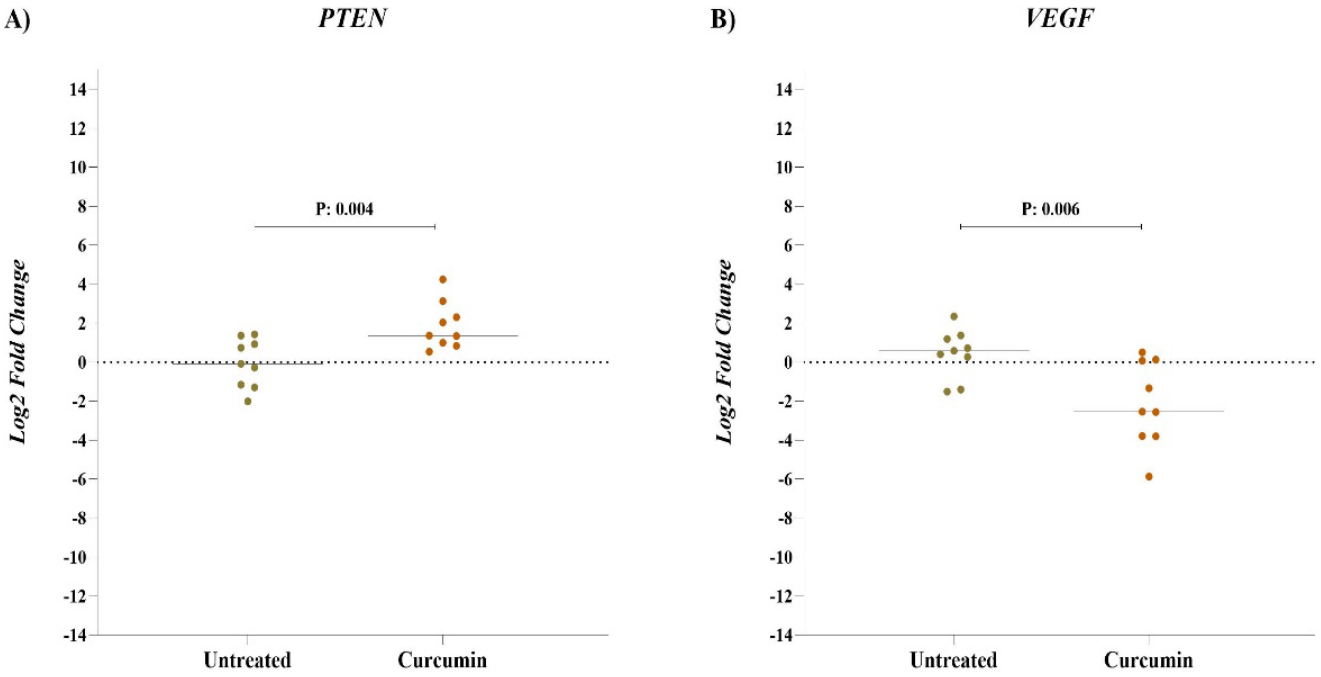

Figure 2. Scatter plots depicting the log2 fold changes in mRNA expression levels of (A) PTEN and (B) VEGF in CaSki cervical cancer cells following 48-hour treatment with 80 µM curcumin compared to untreated controls, as determined by qRT-PCR normalized to GAPDH (n=9 biological replicates per group). Significant upregulation of PTEN (mean log2 fold change: 1.861 ± SD, p=0.004, Welch's t-test) and downregulation of VEGF (mean log2 fold change: -2.137 ± SD, p=0.006) highlight curcumin's modulatory effects on tumor suppression and angiogenesis pathways.

Modulation of miRNA Expression by Curcumin

To further investigate the molecular mechanisms underlying curcumin's effects, the expression levels of four specific miRNAs (miR-21-5p, miR-210-3p, miR-126-3p, and miR-214-3p) were analyzed using qRT-PCR. Data were normalized to U6 small RNA and presented as log2 fold changes (9 replicates per group). miR-21-5p expression showed a trend towards downregulation, with a mean log2 fold change of 0.034 ± SD in untreated cells compared to -1.024 ± SD in curcumin-treated cells (p=0.057, Welch's t-test) [Figure 3A], indicating a decrease of approximately 0.48-fold. miR-210-3p expression did not differ significantly, with a mean log2 fold change of 0.065 ± SD in untreated cells versus -0.767 ± SD in treated cells (p = 0.344, Welch's t-test) [Figure 3B]. Conversely, miR-126-3p exhibited a notable upregulation, with a mean log2 fold change of 0.005 ± SD in untreated cells and 1.674 ± SD in curcumin-treated cells (p=0.003, Welch's t-test) [Figure 3C], representing a significant increase of approximately 3.2-fold. Similarly, miR-214-3p showed a significant increase in expression, with a mean log2 fold change of -0.022 ± SD in untreated cells and 1.669 ± SD in treated cells (p = 0.019, Welch's t-test), although the non-parametric Mann-Whitney U test suggested borderline significance with a p-value of 0.034 [Figure 3D]. These findings demonstrate that curcumin selectively modulates

miRNA expression, particularly promoting the upregulation of tumor-suppressive miR-126-3p, which may play a role in its therapeutic effects in cervical cancer.

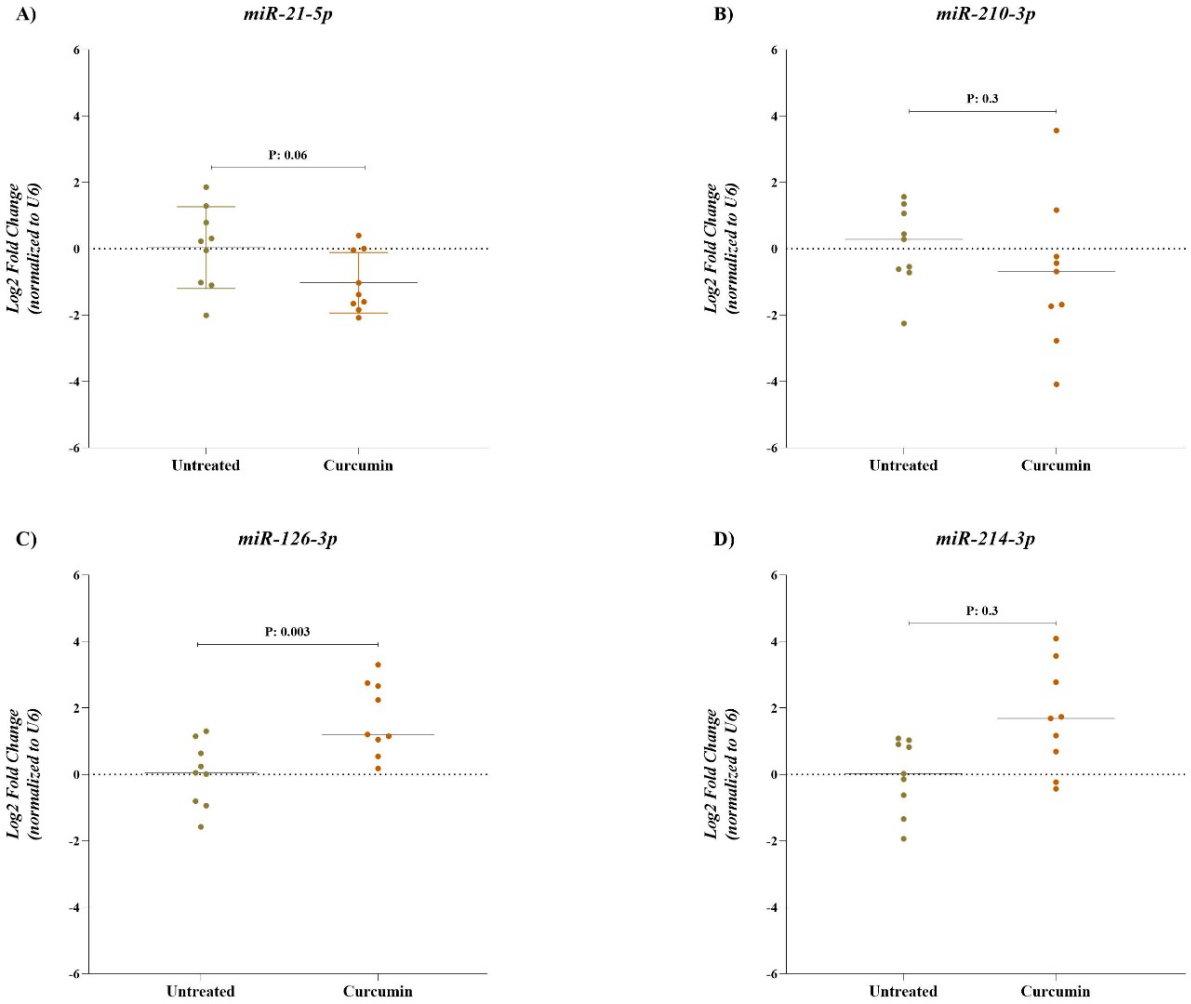

Figure 3. Scatter plots showing the log2 fold changes in miRNA expression levels of (A) miR-21-5p, (B) miR-210-3p, (C) miR-126-3p, and (D) miR-214-3p in CaSki cervical cancer cells after 48-hour exposure to 80 μM curcumin compared to untreated controls, as measured by qRT-PCR normalized to U6 snRNA (n=9 biological replicates per group). Curcumin treatment resulted in a trend toward downregulation of miR-21-5p (mean log2 fold change: -1.024 ± SD, p=0.057), no significant alteration in miR-210-3p (mean log2: -0.767 ± SD, p=0.344), and significant upregulation of miR-126-3p (mean log2: 1.674 ± SD, p=0.003) and miR-214-3p (mean log2: 1.669 ± SD, p=0.019), evaluated using Welch's t-test.

Predictive Correlations Between miRNAs and Target Genes

To explore potential regulatory networks, Pearson correlation analysis was performed on the combined dataset of untreated and curcumin-treated samples (n=18 per parameter). miR-21-5p showed a significant negative correlation with PTEN (r=-0.51, p=0.03) and a significant positive correlation with VEGF (r=0.57, p=0.01) (Figure 4A, B), consistent with its role in oncogenesis by repressing PTEN and promoting VEGF. miR-210-3p exhibited no significant correlations with either PTEN (r=-0.28, p=0.25) or VEGF (r=0.27, p=0.28) [Figure 4C, D]. In contrast, miR-126-3p demonstrated a positive correlation with PTEN (r=0.41, p=0.09) and a significant negative correlation with VEGF (r=-0.49, p=0.03) [Figure 4E, F], supporting its tumor-suppressive role in modulating angiogenesis. miR-214-3p showed a negative correlation with PTEN (r=-0.36, p=0.14) and a non-significant positive correlation with VEGF (r=0.20, p=0.42) [Figure 4G, H]. These correlations provide valuable insights into the miRNA-gene regulatory networks modulated by curcumin, with potential direct interactions between miR-21-5p and PTEN, and miR-126-3p and VEGF, in line with previous studies on curcumin's epigenetic effects in cancer.

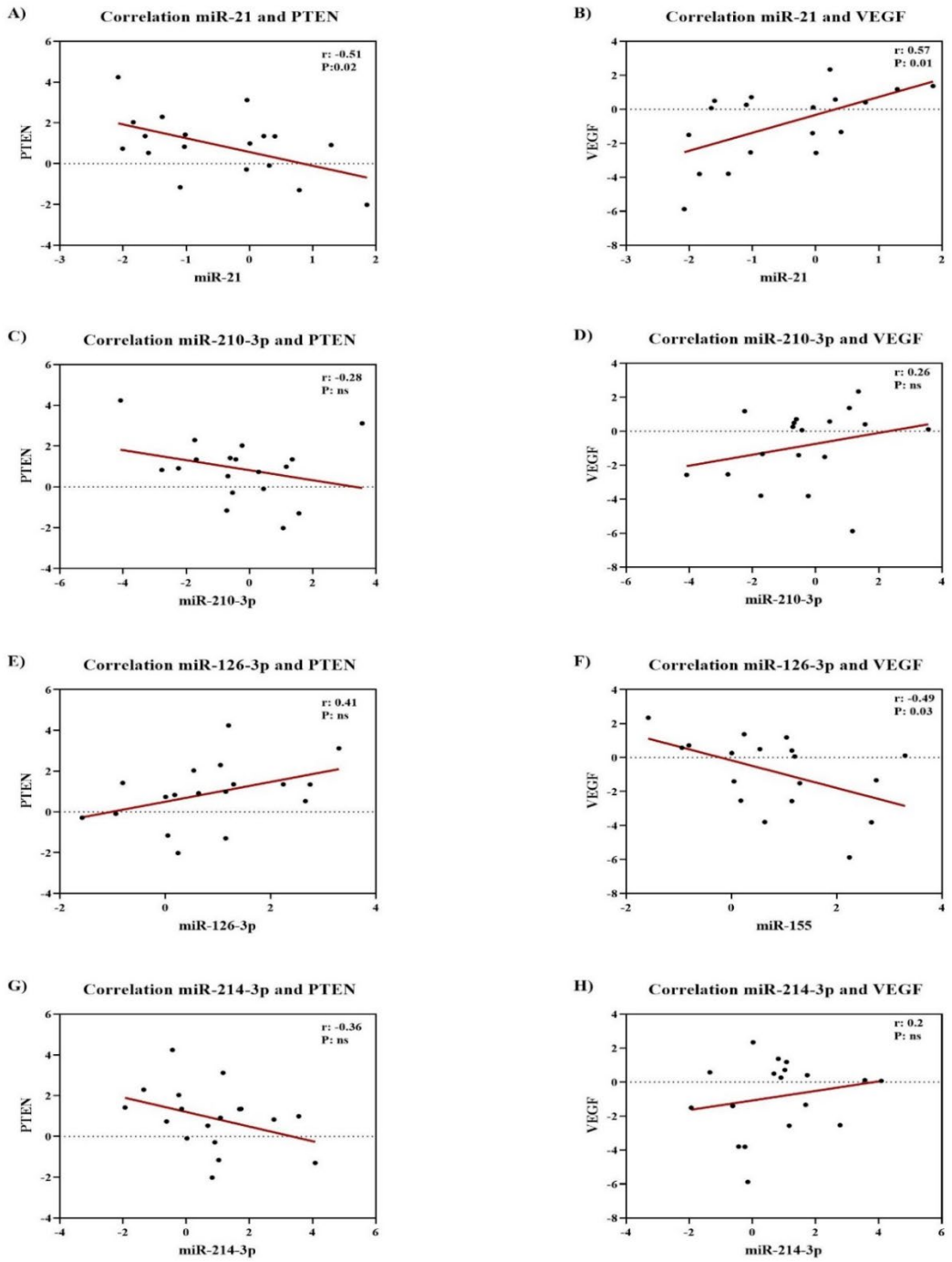

Figure 4. Scatter plots illustrating Pearson correlation analyses between the log2 fold changes in expression levels of (A, B) miR-21-5p, (C, D) miR-210-3p, (E, F) miR-126-3p, and (G, H) miR-214-3p with PTEN and VEGF in combined untreated and curcumin-treated CaSki cervical cancer cells (n=18 samples). Significant correlations include negative association of miR-21-5p with PTEN (r=-0.51, p=0.03) and positive with VEGF (r=0.57, p=0.01), as well as negative association of miR-126-3p with VEGF (r=-0.49, p=0.03), while other relationships were non-significant (ns), highlighting potential regulatory networks in curcumin's anti-cancer mechanisms.

Discussion

The present study demonstrates that curcumin induces cytotoxic effects on HPV-16-positive CaSki cervical cancer cells in a concentration-dependent manner, with an IC50 value of 96 μM following 48 hours of exposure. At a sub-IC50 concentration of 80 μM, curcumin significantly upregulated PTEN mRNA expression by approximately 3.6-fold and downregulated VEGF mRNA to 0.23-fold of control levels, consistent with its known role in modulating the PI3K/Akt pathway. Additionally, curcumin selectively altered miRNA expression profiles: miR-21-5p exhibited a trend toward downregulation (0.48-fold), miR-210-3p remained unchanged, while miR-126-3p and miR-214-3p were significantly upregulated

(both approximately 3.2-fold). Pearson correlation analyses revealed predictive regulatory relationships, including a negative correlation between miR-21-5p and PTEN (r=-0.51, p=0.03) and a positive correlation with VEGF (r=0.57, p=0.01). Furthermore, a positive correlation between miR-126-3p and PTEN (r=0.41, p=0.09) and a negative correlation with VEGF (r=-0.49, p=0.03) were observed. These findings highlight curcumin's potential to epigenetically modulate miRNAs, particularly targeting the PTEN/VEGF axis, and thereby inhibit cervical cancer progression.

Curcumin's cytotoxicity in CaSki cells is consistent with previous reports in cervical cancer models, where concentrations ranging from 30-100 μM induce anti-proliferative effects without causing excessive cell death. The observed IC50 of 96 μM aligns with findings in HeLa and SiHa cells, reinforcing curcumin's dose-dependent inhibition of cell viability through mechanisms such as cell cycle arrest and apoptosis induction. At sub-IC50 concentrations, curcumin's upregulation of PTEN and downregulation of VEGF suggest a shift toward tumor suppression and anti-angiogenesis. PTEN, a critical negative regulator of the PI3K/Akt pathway, is frequently inactivated in cervical cancer, leading to unregulated cell proliferation and survival. Curcumin's ability to restore PTEN expression likely inhibits Akt activation, thereby reducing downstream effectors such as VEGF, a key driver of neovascularization required for tumor growth and metastasis. This mechanism is further supported by in vivo xenograft models, where curcumin suppresses cervical tumor angiogenesis via VEGF inhibition.[33, 35-38]

The selective modulation of miRNAs by curcumin offers valuable insights into its epigenetic anti-cancer mechanisms. The trend toward miR-21-5p downregulation (p=0.057) is particularly noteworthy, as miR-21-5p is a well-established oncomiR in cervical cancer, being overexpressed in HPV-positive tissues and associated with advanced disease stages and poor prognosis. MiR-21-5p targets PTEN, thereby promoting PI3K/Akt activation and VEGF expression, which in turn enhances cellular proliferation and angiogenesis.[39-42] Curcumin's suppression of miR-21-5p is consistent with findings in other cancer models, where it restores PTEN expression, inhibits Akt activation, and disrupts downstream oncogenic signaling. The observed negative correlation between miR-21-5p and PTEN, alongside a positive correlation with VEGF, supports a model in which curcumin mitigates miR-21-5p-mediated repression of PTEN, thereby indirectly attenuating VEGF-driven angiogenesis.[36, 43-45]

The lack of significant change in miR-210-3p expression (p=0.344) is particularly intriguing, as this hypoxia-inducible miRNA is typically upregulated in cervical cancer, where it enhances VEGF expression and promotes angiogenesis under low-oxygen conditions. Curcumin's neutral effect on miR-210-3p may reflect context-specific regulation, potentially influenced by the normoxic conditions of the experimental setup, where the hypoxia-inducible factor-1α (HIF-1α)-mediated induction of miR-210-3p is minimal.[22,46-48] The absence of significant correlations with PTEN and VEGF further suggests that miR-210-3p may not be a central mediator of curcumin's effects in this model. However, it is important to note that hypoxic tumor microenvironments could enhance its role in vivo, potentially altering its contribution to curcumin's therapeutic effects.

In contrast, the significant upregulation of miR-126-3p (p = 0.003) is consistent with its known tumor-suppressive role in cervical cancer, where it inhibits VEGF and reduces endothelial cell proliferation and migration. The positive correlation with PTEN and the negative correlation with VEGF support a model in which curcumin-induced miR-126-3p enhances PTEN-mediated inhibition of the PI3K/Akt pathway, leading to reduced VEGF expression and attenuated angiogenesis.[49-53] This finding aligns with studies in other cancer types, where curcumin exerts anti-angiogenic effects through miRNA modulation.

The upregulation of miR-214-3p (p=0.019) presents a complex scenario, as this miRNA exhibits context-dependent roles in cancer. In some cancer, miR-214-3p is typically oncogenic, as it targets PTEN.[54-59] However, the curcumin-induced increase observed here, along with a negative correlation with PTEN (r=-0.36, p=0.14) and a non-significant positive correlation with VEGF (r=0.20, p=0.42), suggests that miR-214-3p may exhibit tumor-suppressive effects in this model, potentially through

alternative targets such as EZH2 or β-catenin. The borderline significance observed in the Mann-Whitney test (p=0.034) calls for further validation, but these findings underscore the complexity of curcumin's miRNA regulation and its potential for context-dependent therapeutic effects.

Overall, the miRNA-gene correlations reinforce curcumin's role in reprogramming the PTEN/PI3K/Akt/VEGF signaling axis, a critical pathway driving the hallmarks of cervical cancer. By downregulating oncomiRs like miR-21-5p and upregulating tumor suppressors such as miR-126-3p, curcumin may enhance PTEN activity, inhibit Akt, and reduce VEGF expression, collectively hindering tumor growth and angiogenesis.

However, there are limitations to the current study, including its in vitro nature, which may not fully replicate the complex interactions within the tumor microenvironment, and the reliance on a single HPV-16-positive cell line, which may limit the generalizability of the findings to other HPV subtypes. Future research should aim to validate these findings in vivo, investigate potential synergistic effects with chemotherapy, and evaluate miRNA modulation in patient-derived models.

Conclusions

Curcumin modulates specific miRNAs in CaSki cells, with predictive correlations to PTEN upregulation and VEGF downregulation, providing a mechanistic foundation for its anti-cancer effects. These findings support the potential of curcumin as an adjunctive therapy for cervical cancer, warranting further translational studies.

Acknowledgment

None.

Competing interests

The authors declare that they have no competing interests.

Abbreviations

Hypoxia-Inducible Factor 1-alpha: HIF-1α; Human Papillomavirus: HPV; Phosphatidylinositol 3-Kinase: PI3K; Protein Kinase B: Akt; Nuclear Factor kappa-light-chain-enhancer of activated B cells: NF-κB; Mitogen-Activated Protein Kinase: MAPK; microRNAs: miRNAs; 3'-Untranslated Regions: 3'-UTRs; Phosphatase and Tensin Homolog: PTEN; Vascular Endothelial Growth Factor: VEGF; Epithelial-to-Mesenchymal Transition: EMT; American Type Culture Collection: ATCC; Roswell Park Memorial Institute: RPMI; Fetal Bovine Serum: FBS; Ethylenediaminetetraacetic Acid: EDTA; Dimethyl Sulfoxide: DMSO; Polymerase Chain Reaction: PCR; Nicotinamide Adenine Dinucleotide Phosphate: NAD(P)H; Phosphate-Buffered Saline: PBS; Half-Maximal Inhibitory Concentration: IC50; Complementary DNA: cDNA; Quantitative Real-Time PCR: qRT-PCR; Glyceraldehyde-3-Phosphate Dehydrogenase: GAPDH; Locked Nucleic Acid: LNA; Small Nuclear RNA: snRNA; Standard Deviation: SD; Enhancer of Zeste Homolog 2: EZH2.

Authors' contributions

All authors read and approved the final manuscript. All authors take responsibility for the integrity of the data and the accuracy of the data analysis.

Funding

None.

Role of the funding source

None.

Availability of data and materials

The data used in this study are available from the corresponding author on request.

Ethics approval and consent to participate

The study was conducted in accordance with the Declaration of Helsinki.

Consent for publication

By submitting this document, the authors declare their consent for the final accepted version of the manuscript to be considered for publication.

References

1. Li Z, Liu P, Yin A, et al. Global landscape of cervical cancer incidence and mortality in 2022 and predictions to 2030: The urgent need to address inequalities in cervical cancer. Int J Cancer. 2025; 157 (2): 288-97. doi:10.7150/jca.101420 PMid:40026066
2. Wu J, Jin Q, Zhang Y, et al. Global burden of cervical cancer: current estimates, temporal trend and future projections based on the GLOBOCAN 2022. J Natl Cancer Cent. 2025;5(3):322-9. doi:10.1016/j.jncc.2024.11.006 PMid:40693230 PMCid:PMC12276544
3. Siegel RL, Kratzer TB, Giaquinto AN, et al. Cancer statistics, 2025. CA Cancer J Clin. 2025;75(1):10. doi:10.3322/caac.21871 PMid:39817679 PMCid:PMC11745215
4. Sadri Nahand J, Moghoofei M, Salmaninejad A, et al. Pathogenic role of

exosomes and microRNAs in HPV-mediated inflammation and cervical cancer: a review. Int J Cancer. 2020;146(2):305-20. doi:10.1002/ijc.32688 PMid:31566705 PMCid:PMC6999596

5. Hussen BM, Ahmadi G, Marzban H, et al. The role of HPV gene expression and selected cellular MiRNAs in lung cancer development. Microb Pathog. 2021;150:104692. doi:10.1016/j.micpath.2020.104692 PMid:33301856
6. Nahand JS, Khanaliha K, Mirzaei H, et al. Possible role of HPV/EBV coinfection in anoikis resistance and development in prostate cancer. BMC Cancer. 2021;21(1):926. doi:10.1186/s12885-021-08658-y PMid:34399719 PMCid:PMC8369687
7. Shiri Aghbash P, Rasizadeh R, Sadri Nahand J, et al. The role of immune cells and inflammasomes in Modulating cytokine responses in HPV-Related cervical cancer. Int Immunopharmacol. 2025;145:113625. doi:10.1016/j.intimp.2024.113625 PMid:39637578
8. Rasizadeh R, Shiri Aghbash P, Mokhtarzadeh A, et al. Novel strategies in HPV-16-related cervical cancer treatment: An in vitro study of combined siRNA-E5 with oxaliplatin and ifosfamide chemotherapy. Gene. 2025;932:148904. doi:10.1016/j.gene.2024.148904 PMid:39218415
9. Taghizadieh M, Kalantari M, Bakhshali R, et al. To be or not to be: navigating the influence of MicroRNAs on cervical cancer cell death. Cancer Cell Int. 2025;25(1):153. doi:10.1186/s12935-025-03786-y PMid:40251577 PMCid:PMC12008905
10. Nahand JS, Rabiei N, Fathazam R, et al. Oncogenic viruses and chemoresistance: What do we know? Pharmacol Res. 2021;170:105730. doi:10.1016/j.phrs.2021.105730 PMid:34119621
11. Bayat M, Golestani S, Motlaghzadeh S, et al. War or peace: Viruses and metastasis. Biochim Biophys Acta Rev Cancer. 2024;1879(6): 189179. doi:10.1016/j.bbcan.2024.189179 PMid:39299491
12. Zaman MS, Chauhan N, Yallapu MM, et al. Curcumin Nanoformulation for Cervical Cancer Treatment. Sci Rep. 2016; 6(1): 20051. doi:10.1038/srep20051 PMid:26837852 PMCid:PMC4738284
13. Ming T, Tao Q, Tang S, et al. Curcumin: An epigenetic regulator and its application in cancer. Biomed Pharmacother. 2022;156: 113956. doi:10.1016/j.biopha.2022.113956 PMid:36411666
14. Zhou S, Zhang S, Shen H, et al. Curcumin inhibits cancer progression through regulating expression of microRNAs. Tumour Biol. 2017;39(2): 1010428317691680. doi:10.1177/1010428317691680 PMid:28222667
15. Asiri A, Bokahri BT, Sadaf, et al. Curcumin, EGCG and apigenin in cervical cancer: mechanistic insights and therapeutic potential. Front Pharmacol. 2025;16. doi:10.3389/fphar.2025.1592395 PMid:40667502 PMCid:PMC12259677
16. Mirzaei H, Rahimian N, Mirzaei HR, et al. MicroRNA biogenesis and function. In: Mirzaei H, Rahimian N, Hamblin MR, eds. Exosomes and MicroRNAs in Biomedical Science. Springer; 2022:1-9. doi:10.1007/978-3-031-79177-2_1
17. Rahimian N, Nahand JS, Hamblin MR, et al. Exosomal MicroRNA Profiling. In: Rani S, ed. MicroRNA Profiling: Methods and Protocols. Springer US; 2023:13-47. doi:10.1007/978-1-0716-2823-2_2 PMid:36441452
18. Bayat M, Sadri Nahand J. Exosomal miRNAs: the tumor's trojan horse in selective metastasis. Mol Cancer. 2024;23(1):167. doi:10.1186/s12943-024-02081-0 PMid:39164756 PMCid:PMC11334467
19. Chen J, Xu T, Chen C. The critical roles of miR-21 in anti-cancer effects of curcumin. Ann Transl Med. 2015;3(21):330.
20. Xu J, Zhang W, Lv Q, et al. Overexpression of miR-21 promotes the proliferation and migration of cervical cancer cells via the inhibition of PTEN. Oncol Rep. 2015;33(6):3108-16. doi:10.3892/or.2015.3931 PMid:25963606
21. Ghafouri-Fard S, Abak A, Shoorei H, et al. Regulatory role of microRNAs on PTEN signaling. Biomed Pharmacother. 2021; 133: 110986. doi:10.1016/j.biopha.2020.110986 PMid:33166764
22. Lu WJ, Liang HB, Li YF, et al. MicroRNA-210-3p Targets RGMA to Enhance the Angiogenic Functions of Endothelial Progenitor Cells Under Hypoxic Conditions. Front Cell Neurosci. 2019;13:223. doi:10.3389/fncel.2019.00223 PMid:31164807 PMCid:PMC6536652
23. Cao G, Fan P, Ma R, et al. MiR-210 regulates lung adenocarcinoma by targeting HIF-1α. Heliyon. 2023;9(5):e16079. doi:10.1016/j.heliyon.2023.e16079 PMid:37215862 PMCid:PMC10192744
24. Zhao N, Na K, Sun W, et al. Plasma microRNA-210 is associated with VEGF-A and EphrinA3 and relates to coronary collateral circulation in patients with coronary heart disease: a cross-sectional study. BMC Cardiovasc Disord. 2025;25(1):547. doi:10.1186/s12872-025-05013-y PMid:40717103 PMCid:PMC12302828
25. Du C, Lv Z, Cao L, et al. MiR-126-3p suppresses tumor metastasis and angiogenesis of hepatocellular carcinoma by targeting LRP6 and PIK3R2. J Transl Med. 2014;12:259. doi:10.1186/s12967-014-0259-1 PMid:25240815 PMCid:PMC4189615
26. Guo B, Gu J, Zhuang T, et al. MicroRNA-126: From biology to therapeutics. Biomed Pharmacother. 2025;185:117953. doi:10.1016/j.biopha.2025.117953 PMid:40036996
27. Caporali S, Amaro A, Levati L, et al. miR-126-3p down-regulation contributes to dabrafenib acquired resistance in melanoma by up-regulating ADAM9 and VEGF-A. J Exp Clin Cancer Res. 2019;38 (1):272. doi:10.1186/s13046-019-1238-4 PMid:31227006 PMCid:PMC6588909
28. Akaray I, Ozal SA, Sancar H, et al. miR-124, miR-126-3p, and miR-200b: Potential therapeutic targets for VEGF-mediated complications in proliferative diabetic retinopathy. Indian J Ophthalmol. 2025;73(6):886-92. doi:10.4103/IJO.IJO_1791_24 PMid:39728608 PMCid:PMC12178365
29. Chen Z, Deng X, Lu Y, et al. Role of miRNA-214-3p in cancer (Review). Oncol Rep. 2025;54(4):123. doi:10.3892/or.2025.8957 PMid:40747717 PMCid:PMC12340666
30. Wang X, Xu J, Hua F, et al. MiR-214-3p suppresses cervical cancer cell metastasis by downregulating THBS2. Cell Mol Biol (Noisy-le-grand). 2023;69(9):195-200. doi:10.14715/cmb/2023.69.9.30 PMid:37807313
31. Sukmana BI, Al-Hawary SIS, Abosaooda M, et al. A thorough and current study of miR-214-related targets in cancer. Pathol Res Pract. 2023;249:154770. doi:10.1016/j.prp.2023.154770 PMid:37660658
32. Eslami M, Khazeni S, Khanaghah XM, et al. MiRNA-related metastasis in oral cancer: moving and shaking. Cancer Cell Int. 2023;23(1):182. doi:10.1186/s12935-023-03022-5 PMid:37635248 PMCid:PMC10463971
33. Pourhanifeh MH, Darvish M, Tabatabaeian J, et al. Therapeutic role of curcumin and its novel formulations in gynecological cancers. J Ovarian Res. 2020;13(1):130. doi:10.1186/s13048-020-00731-7 Mid:33148295 PMCid:PMC7643381
34. Bhattacharjee R, Das SS, Biswal SS, et al. Mechanistic role of HPV-associated early proteins in cervical cancer: Molecular pathways and targeted therapeutic strategies. Crit Rev Oncol Hematol. 2022; 174: 103675. doi:10.1016/j.critrevonc.2022.103675 PMid:35381343
35. Liu Y, Sun H, Makabel B, et al. The targeting of non-coding RNAs by curcumin: Facts and hopes for cancer therapy (Review). Oncol Rep. 2019;42(1):20-34. doi:10.3892/or.2019.7148 PMid:31059075 PMCid:PMC6549103
36. Zoi V, Kyritsis AP, Galani V, et al. The Role of Curcumin in Cancer: A Focus on the PI3K/Akt Pathway. Cancers (Basel). 2024;16(8). doi:10.3390/cancers16081554 PMid:38672636 PMCid:PMC11048628
37. Rahmani AH, Al Zohairy MA, Aly SM, et al. Curcumin: a potential candidate in prevention of cancer via modulation of molecular pathways. Biomed Res Int. 2014;2014:761608. doi:10.1155/2014/761608 PMid:25295272 PMCid:PMC4176907
38. Ameer SF, Mohamed MY, Elzubair QA, et al. Curcumin as a novel therapeutic candidate for cancer: can this natural compound revolutionize cancer treatment? Front Oncol. 2024;14. doi:10.3389/fonc.2024.1438040 PMid:39507759 PMCid:PMC11537944
39. Chen Y, Su C, Cai Y, et al. miR-21 promotes cervical cancer by regulating

NTF3. Sci Rep. 2025;15(1):2442. doi:10.1038/s41598-025-85888-1 PMid:39828780 PMCid:PMC11743774
40. Aguilar-Martínez SY, Campos-Viguri GE, Medina-García SE, et al. MiR-21 Regulates Growth and Migration of Cervical Cancer Cells by RECK Signaling Pathway. Int J Mol Sci. 2024;25(7). doi:10.3390/ijms25074086 PMid:38612895 PMCid:PMC11012906
41. Mitra T, Prusty M, Elangovan S. Identification and validation of miR-21 key genes in cervical cancer through an integrated bioinformatics approach. Comput Biol Chem. 2024;113:108280. doi:10.1016/j.compbiolchem.2024.108280 PMid:39571453
42. Tang Y, Zhao Y, Ran J, et al. MicroRNA-21 promotes cell metastasis in cervical cancer through modulating epithelial-mesenchymal transition. Oncol Lett. 2020;19 (4): 3289-95. doi:10.3892/ol.2020.11438 PMid:32256824 PMCid:PMC7074379
43. Chauhan P, Pramodh S, Hussain A, et al. Understanding the role of miRNAs in cervical cancer pathogenesis and therapeutic responses. Front Cell Dev Biol. 2024;12:1397945. doi:10.3389/fcell.2024.1397945 PMid:39263322 PMCid:PMC11387185
44. Endale HT, Mariye YF, Negash HK, et al. MiRNA in cervical cancer: Diagnosis to therapy: Systematic review. Heliyon. 2024;10(3): e24398. doi:10.1016/j.heliyon.2024.e24398 PMid:38317930 PMCid:PMC10839805
45. He Y, Lin J, Ding Y, et al. A systematic study on dysregulated micro RNA s in cervical cancer development. Int J Cancer. 2016;138(6):1312-27. doi:10.1002/ijc.29618 PMid:26032913
46. Wang H, Wang L, Zhou X, et al. OSCC Exosomes Regulate miR-210-3p Targeting EFNA3 to Promote Oral Cancer Angiogenesis through the PI3K/AKT Pathway. Biomed Res Int. 2020;2020: 2125656. doi:10.1155/2020/2125656 PMid:32695810 PMCid:PMC7368228
47. Yang Y, Zhang J, Xia T, et al. MicroRNA-210 promotes cancer angiogenesis by targeting fibroblast growth factor receptor-like 1 in hepatocellular carcinoma. Oncol Rep. 2016;36(5):2553-62. doi:10.3892/or.2016.5129 PMid:27666683
48. Pasculli B, Barbano R, Rendina M, et al. Hsa-miR-210-3p expression in breast cancer and its putative association with worse outcome in patients treated with Docetaxel. Sci Rep. 2019;9(1):14913. doi:10.1038/s41598-019-51581-3 PMid:31624308 PMCid:PMC6797767
49. Lu G, Wu X, Zhao Z, et al. MicroRNA-126 regulates the phosphatidylinositol-3 kinase (PI3K)/protein kinase B (AKT) pathway in SLK cells in vitro and the expression of its pathway members in Kaposi's sarcoma tissue. Medicine (Baltimore). 2018; 97(35):e11855. doi:10.1097/MD.0000000000011855 PMid:30170375 PMCid:PMC6392886
50. Di Paolo D, Pontis F, Moro M, et al. Cotargeting of miR-126-3p and miR-221-3p inhibits PIK3R2 and PTEN, reducing lung cancer growth and metastasis by blocking AKT and CXCR4 signalling. Mol Oncol. 2021;15(11):2969-88. doi:10.1002/1878-0261.13036 PMid:34107168 PMCid:PMC8564655
51. Ichikawa R, Kawasaki R, Iwata A, et al. MicroRNA-126-3p suppresses HeLa cell proliferation, migration and invasion, and increases apoptosis via the PI3K/PDK1/AKT pathway. Oncol Rep. 2020; 43(4):1300-8. doi:10.3892/or.2020.7512 PMid:32323808 PMCid:PMC7057934
52. Song L, Li D, Gu Y, et al. MicroRNA-126 Targeting PIK3R2 Inhibits NSCLC A549 Cell Proliferation, Migration, and Invasion by Regulation of PTEN/PI3K/AKT Pathway. Clin Lung Cancer. 2016;17(5):e65-e75. doi:10.1016/j.cllc.2016.03.012 PMid:27236384
53. Jalil AT, Abdulhadi MA, Al-Ameer LR, et al. The emerging role of microRNA-126 as a potential therapeutic target in cancer: a comprehensive review. Pathol Res Pract. 2023;248:154631. doi:10.1016/j.prp.2023.154631 PMid:37393667
54. Yang Y, Liu Y, Li G, et al. microRNA-214 suppresses the growth of cervical cancer cells by targeting EZH2. Oncol Lett. 2018; 16(5): 5679-86. doi:10.3892/ol.2018.9363 PMid:30344723 PMCid:PMC6176260
55. Penna E, Orso F, Taverna D. miR-214 as a Key Hub that Controls Cancer Networks: Small Player, Multiple Functions. J Invest Dermatol. 2015;135(4):960-9. doi:10.1038/jid.2014.479 PMid:25501033
56. Fang YY, Tan MR, Zhou J, et al. miR-214-3p inhibits epithelial-to-mesenchymal transition and metastasis of endometrial cancer cells by targeting TWIST1. Onco Targets Ther. 2019;12:9449-58. doi:10.2147/OTT.S181037 PMCid:PMC6875683
57. Schwarzenbach H, Milde-Langosch K, Steinbach B, et al. Diagnostic potential of PTEN-targeting miR-214 in the blood of breast cancer patients. Breast Cancer Res Treat. 2012;134(3): 933-41. doi:10.1007/s10549-012-1988-6 PMid:22350790
58. Yang TS, Yang XH, Wang XD, et al. MiR-214 regulate gastric cancer cell proliferation, migration and invasion by targeting PTEN. Cancer Cell Int. 2013;13(1):68. doi:10.1186/1475-2867-13-68 PMid:23834902 PMCid:PMC3716801
59. Liu J, Chen W, Zhang H, et al. miR-214 targets the PTEN-mediated PI3K/Akt signaling pathway and regulates cell proliferation and apoptosis in ovarian cancer. Oncol Lett. 2017; 14(5):5711-8. doi:10.3892/ol.2017.6953 PMid:29113199 PMCid:PMC5661372
60. Ma J, Sun X, Wang Y, et al. Fibroblast-derived CXCL12 regulates PTEN expression and is associated with the proliferation and invasion of colon cancer cells via PI3k/Akt signaling. Cell Commun Signal. 2019;17(1): 119. doi:10.1186/s12964-019-0432-5 PMid:31500630 PMCid:PMC6734448
61. Medford AR, Douglas SK, Godinho SI, et al. Vascular Endothelial Growth Factor (VEGF) isoform expression and activity in human and murine lung injury. Respir Res. 2009;10(1):27. doi:10.1186/1465-9921-10-27 PMid:19358726 PMCid:PMC2674417
62. Kwon N, Lee KE, Singh M, et al. Suitable primers for GAPDH reference gene amplification in quantitative RT-PCR analysis of human gene expression. Gene Rep. 2021;24:101272. doi:10.1016/j.genrep.2021.101272
63. Zhang WY, Wang HB, Deng CY. Effects of miR-214-5p and miR-21-5p in hypoxic endometrial epithelial-cell-derived exosomes on human umbilical cord mesenchymal stem cells. World J Stem Cells. 2024; 16 (11):906-25. doi:10.4252/wjsc.v16.i11.906 PMid:39619875 PMCid:PMC11606348
64. Hayder H, Fu G, Nadeem L, et al. Overexpression of miR-210-3p Impairs Extravillous Trophoblast Functions Associated with Uterine Spiral Artery Remodeling. Int J Mol Sci. 2021;22(8). doi:10.3390/ijms22083961 PMid:33921262 PMCid:PMC8069107
65. Kang K, Zhang X, Liu H, et al. A novel real-time PCR assay of microRNAs using S-Poly (T), a specific oligo (dT) reverse transcription primer with excellent sensitivity and specificity. PLoS One. 2012; 7 (11): e48536. doi:10.1371/journal.pone.0048536 PMid:23152780 PMCid:PMC3496722
66. Niu Y, Zhang L, Qiu H, et al. An improved method for detecting circulating microRNAs with S-Poly(T) Plus real-time PCR. Sci Rep. 2015;5 (1):15100. doi:10.1038/srep15100 PMid:26459910 PMCid:PMC4602224
67. Cai H, Miao M, Wang Z. miR-214-3p promotes the proliferation, migration and invasion of osteosarcoma cells by targeting CADM1. Oncol Lett. 2018;16(2):2620-8. doi:10.3892/ol.2018.8927 PMid:30013657 PMCid:PMC6036594
68. Mabin JW, Lewis PW, Brow DA, et al. Human spliceosomal snRNA sequence variants generate variant spliceosomes. RNA. 2021;27(10):1186-203. doi:10.1261/rna.078768.121 PMid:34234030 PMCid:PMC8457000

Cite this article as:
Mohammadi P. Curcumin-Mediated Modulation of miR-21-5p and miR-126-3p Enhances PTEN Expression and Suppresses VEGF in Caski Cell line. J Cancer Res Pharmacol. 2025; 1(2): 89-100. doi: 10.22034/jcrph.2025.559607.1015